J. Biochem. 129, 173–178 (2001)

Temperature Dependence of the Enzyme-Substrate Recognition Mechanism[1]

Hideaki Ura,[*] Kazuaki Harata,[†] Ikuo Matsui,[†] and Seiki Kuramitsu[*,‡,§,2]

[*]Department of Biology, Graduate School of Science, Osaka University, Toyonaka, Osaka 560-0043; [†]National Institute of Bioscience and Human-Technology, Tsukuba, Ibaraki 305-8566; [‡]Genomic Sciences Center, RIKEN Yokohama Institute, 1-7-22 Suehiro-cho, Tsurumi, Yokohama 230-0045; and [§]Harima Institute/SPring-8, 1-1-1 Koto, Mikazuki-cho, Sayo-gun, Hyogo 679-5148

Received September 28, 2000; accepted November 8, 2000

We determined the crystal structure of the liganded form of α-aminotransferase from a hyperthermophile, *Pyrococcus horikoshii*. This hyperthermophilic enzyme did not show domain movement upon binding of an acidic substrate, glutamate, except for a small movement of the α-helix from Glu16 to Ala25. The ω-carboxyl group of the acidic substrate was recognized by Tyr70* without its side-chain movement, but not by positively charged Arg or Lys. Compared with the homologous enzymes from *Thermus thermophilus* HB8 and *Escherichia coli*, it was suggested that the more thermophilic the enzyme is, the smaller the domain movement is. This rule seems to be applicable to many other enzymes already reported.

Key words: aminotransferase, domain movement, hyperthermophilic enzyme, *Pyrococcus horikoshii*, substrate recognition.

The thermostability of thermophilic enzymes has been extensively studied, and it has been suggested that the forces contributing to their thermostability are increases in electrostatic interactions, hydrogen bonding, and packing (*2–9* and references therein). Usually there are no critical residues for increasing the thermal stability of a protein, but rather cumulative small contributions of many residues. However, the temperature dependence of the substrate recognition mechanism remains to be elucidated.

α-Aminotransferases are vitamin B6 enzymes that use an acidic substrate, glutamate, as a common amino donor substrate. Aspartate aminotransferase from the mesophile *Escherichia coli* (EcAT) (*10*, *11*; Fig. 1c) consists of two domains (see the circles in Fig. 1a), which close upon substrate binding (in Figs. 1 and 2, the substrate-free form is colored gray). Recently, we were able to estimate the free energy required for domain movement by means of kinetic studies in a series of aliphatic substrates and corresponding crystallographic studies (*12*). Upon binding of the acidic substrate, the side chain of Arg292* largely moves into the active site to create bifurcated hydrogen bonds and an electrostatic interaction with the distal carboxylate (ω-carboxylate) group of the bound acidic substrate (Fig. 2c).

The aspartate aminotransferase from an extreme thermophile, *Thermus thermophilus* HB8 (TtAT), is a homologue of EcAT. Although the amino acid identity between TtAT and EcAT is 16%, the amino acid residues critical for the conformation, including the residues in the active site, are well conserved (*13*), and the overall conformation of TtAT (Fig. 1b) is very similar to that of EcAT (Fig. 1c).

No large domain movement is observed upon binding of a substrate to TtAT. The single N-terminal α-helix consisting of Lys13 to Val30 approaches the bound substrate and closes the active site (*14*). Ser15 and Thr17 in the N-terminal region of the α-helix interact with one of the carboxylate oxygen atoms of the bound acidic substrate, and Lys109 interacts with another oxygen atom without movement of its side chain (Fig. 2b).

Despite its name, the aromatic amino acid aminotransferase from a hyperthermophile, *Pyrococcus horikoshii* (PhAT), is very similar to TtAT and EcAT. The amino acid sequence identity between PhAT and TtAT is 41%, and both PhAT and TtAT exhibit 16% identity with EcAT. We recently determined the three-dimensional structure of the unliganded form of PhAT (*15*), the overall conformation (Fig. 1a) being found to be almost identical to those of TtAT and EcAT (Fig. 1, b and c).

PhAT is highly active toward glutamate (*15*), as in the case of TtAT and EcAT, but the key positive residue observed for TtAT and EcAT for recognition of an acidic substrate seems not to be present in PhAT (*15*). As the absence of a positive charge seems rather curious, we determined the crystal structure of PhAT complexed with a glutamate

[1]This work was supported in part by the TARA (Tsukuba Advanced Research Alliance) Sakabe project and by Grants-in-Aid for Scientific Research (Nos. 11878118 and 11169224) from the Ministry of Education, Science, Sports and Culture of Japan, and a research grant from the Japan Society for the Promotion of Science ("Research for the Future" Program, No. JSPS-RFTF96L00506). The coordinates for unliganded and glutamate forms of PhAT have been deposited in the RSCB Protein Data Bank as entries 1GD9 and 1GDE, respectively.

[2]To whom correspondence should be addressed. Tel: +81-6-6850-5433, Fax: +81-6-6850-5442, E-mail: kuramitu@bio.sci.osaka-u.ac.jp

Abbreviations: PhAT, aromatic amino acid aminotransferase from *Pyrococcus horikoshii*; TtAT, aspartate aminotransferase from *Thermus thermophilus* HB8; EcAT, aspartate aminotransferase from *Escherichia coli*; Arg292*. The amino acid residues are numbered according to the sequence of porcine cytosolic aspartate aminotransferase (*1*). *indicates the residue belonging to another subunit of the dimer.

analog. These homologous α-aminotransferases with different optimum temperatures suggest a general rule for the temperature dependence of enzyme-substrate recognition.

MATERIALS AND METHODS

Enzyme Preparation—Overexpression and purification of PhAT were performed as described previously (*15*).

Construction of the N-5′-Phosphopyridoxyl-L-Glutamate Form of PhAT—We first attempted to prepare PhAT complexed with glutarate or 2OG, respectively, by soaking the substrate analog for crystallization or cocrystallization, but were unsuccessful. In order to mimic the enzyme-substrate complex, we synthesized a cofactor-substrate analog, *N*-5′-phosphopyridoxyl-L-glutamate (*16*), and prepared a complex of the analog and the apoenzyme. *N*-5′-Phosphopyridoxyl-L-glutamate was synthesized as follows: 2 mmol of PLP and L-glutamate were dissolved in H_2O, and the pH was adjusted to 9.3. The solution was then treated with 0.1 M $NaBH_4$ for 8 h. The decolorized solution was acidified with formic acid, chromatographed on DOWEX 1-X8 anion-exchange resin (bed volume, 150 ml), and then eluted with a linear gradient of 0.2–4.0 M formic acid. The second peak showing absorbance at 330 nm was collected and freeze-dried.

To obtain the apoenzyme, the PMP form of PhAT was treated with 50 mM K_2HPO_4 (pH 11.3) for 40 min at 25°C. The PMP that dissociated from the enzyme was washed out with the same buffer using a Centriprep YM-30, this treatment being repeated until the coenzyme was completely removed. To this apoenzyme, a 5-fold final concentration of *N*-5′-phosphopyridoxyl-L-glutamate was added, followed by incubation for 60 min at 25°C to obtain the holoenzyme. To remove free *N*-5′-phosphopyridoxyl-L-glutamate, anion-exchange chromatography was performed on Mono Q HR 5/5 (Pharmacia Biotech). The peak fraction was washed with 5 mM HEPES (pH 8.0) containing 10 mM KCl, and the holoenzyme obtained was concentrated to 0.2 mM.

Crystallization, Data Collection, and Refinement of PhAT—The crystallization of PhAT was performed by the hanging-drop vapor diffusion method at 20°C using 3 M 1,6-hexane-di-ol, 100 mM HEPES (pH 7.5), and 10 mM $MgCl_2$ as the precipitant solutions (*15*) for the unliganded and *N*-5′-phosphopyridoxyl-L-glutamate forms. The crystals were grown at 20°C for 3–7 days. The crystals were picked up using a loop made from fine thread and then were flash-frozen at 100 K on a goniometer in a stream of cold nitrogen generated by a Cryostream Cooler (Oxford Cryosystems). Freezing caused a 10% decrease in the unit cell volume compared with that at room temperature (*15*). X-ray diffraction data for all forms of PhAT were collected on the BL6A station at the Photon Factory, KEK (Tsukuba), using an X-ray beam of 1.0 Å wavelength and an ADSC Quantum 4R CCD detector. No significant radiation damage was observed during data collection. Images were integrated with the MOSFLM package (*17*), and subsequent data processing was performed with the CCP4 package (*18*). The details of the data collection and processing statistics are given in Table I.

Due to the large change in the unit cell volume, repositioning of the previously reported structure of PhAT (*15*; PDB entry, 1DJU) in the new unit cell by rigid body refinement with XPLOR version 3.851 (*19*) was unsuccessful. Therefore, the initial structure of the unliganded form was determined by molecular replacement with AMoRe (*20*), using the previously reported structure without water molecules. The model was constructed from the dimeric molecule. Data between 15 and 4 Å were included for both the rotation and translation functions. A rotational search followed by Patterson correlation refinement gave two distinct solutions, which resulted in translational solutions of one dimer in the asymmetric unit with an R_{factor} ($= \Sigma ||F_{obs}|-|F_{calc}|| / \Sigma|F_{obs}|$) of 33.1%. The starting point for the *N*-5′-phosphopyridoxyl-L-glutamate form of PhAT was the unliganded form refined at cryogenic temperature. These models were refined by cycles of refinement and manual adjustment using standard XPLOR (*21*, *22*) simulated annealing, energy minimization, and individual B-factor refinement protocols with the parameter files PARHCSDX.PRO (*23*) and program O (*24*). The positions of the oxygen atoms of the water molecules were automatically picked up on the basis of the peak heights and distance criteria from $2F_o–F_c$ difference Fourier maps after every refinement cycle. The introduced water molecules were examined with omit-refined $2F_o–F_c$ maps in the subsequent refinement stage. When the temperature factors of the water molecules became greater than 50 Å^2, the water molecules were removed from the structural models. The alternative refinement cycles were performed until no further improvement in structure and statistics was obtained. The final models for the unliganded and *N*-5′-phosphopyridoxyl-L-glutamate forms included 412 and 394 water molecules, respectively. The statistics of the structural models are summarized in Table I.

TABLE I. **Data collection and refinement statistics.**

	PLP form	*N*-5′-Phosphopyridoxyl-L-glutamate form
Source (Å)	1.0	1.0
Temperature (K)	100	100
Diffraction data		
Space group	$P2_12_12_1$	$P2_12_12_1$
Lattice constants (Å)		
a	59.67	59.33
b	122.28	121.90
c	127.17	127.01
Resolution (Å)	1.8	1.8
Observations	272,833	309,808
Unique reflections	83,030	84,494
Completeness (%)	96.0	98.6
R_{merge}[a] (%)	8.6	5.3
Refinement		
Resolution limits (Å)	8.0–1.8	8.0–1.8
R_{factor}[b] (%)	21.0	19.8
R_{free}[c] (%)	24.2	23.0
Deviations		
Bond length (Å)	0.008	0.010
Bond angles (deg)	1.47	1.64
Dihedral angles (deg)	23.53	23.18
Improper angles (deg)	1.34	1.39
B-factors		
Average main chains (Å^2)	9.82	11.98
Average side chains (Å^2)	8.72	10.09
Average cofactors (Å^2)	13.04	19.20
Average waters (Å^2)	8.69	7.60

[a] $R_{merge} = \Sigma_{hkl} \Sigma_i |I_{hkl,i} - \langle I_{hkl} \rangle| / \Sigma_{hkl} \Sigma_i I_{hkl,i}$ where I represents the observed intensity and $\langle I \rangle$ the mean intensity for multiple measurements. [b] $R_{factor} = \Sigma ||F_{obs}| - |F_{calc}|| / \Sigma |F_{obs}|$. [c] R_{free} was monitored with 10% of the reflection data excluded from the refinement.

Stereochemistry analysis with PROCHECK (*25*) showed that all the main chain atoms except Thr296 fell within the generously allowed regions of the Ramachandran plot for all structures.

All molecular images were produced using Raster3D (*26*) and Molscript (*27*).

RESULTS

Structural Changes upon Substrate Binding to PhAT—The crystal structure of the ligand-free PhAT was analyzed at a resolution of 1.8 Å, which is better than the previous resolution of 2.1 Å (*15*). The overall structure of PhAT is

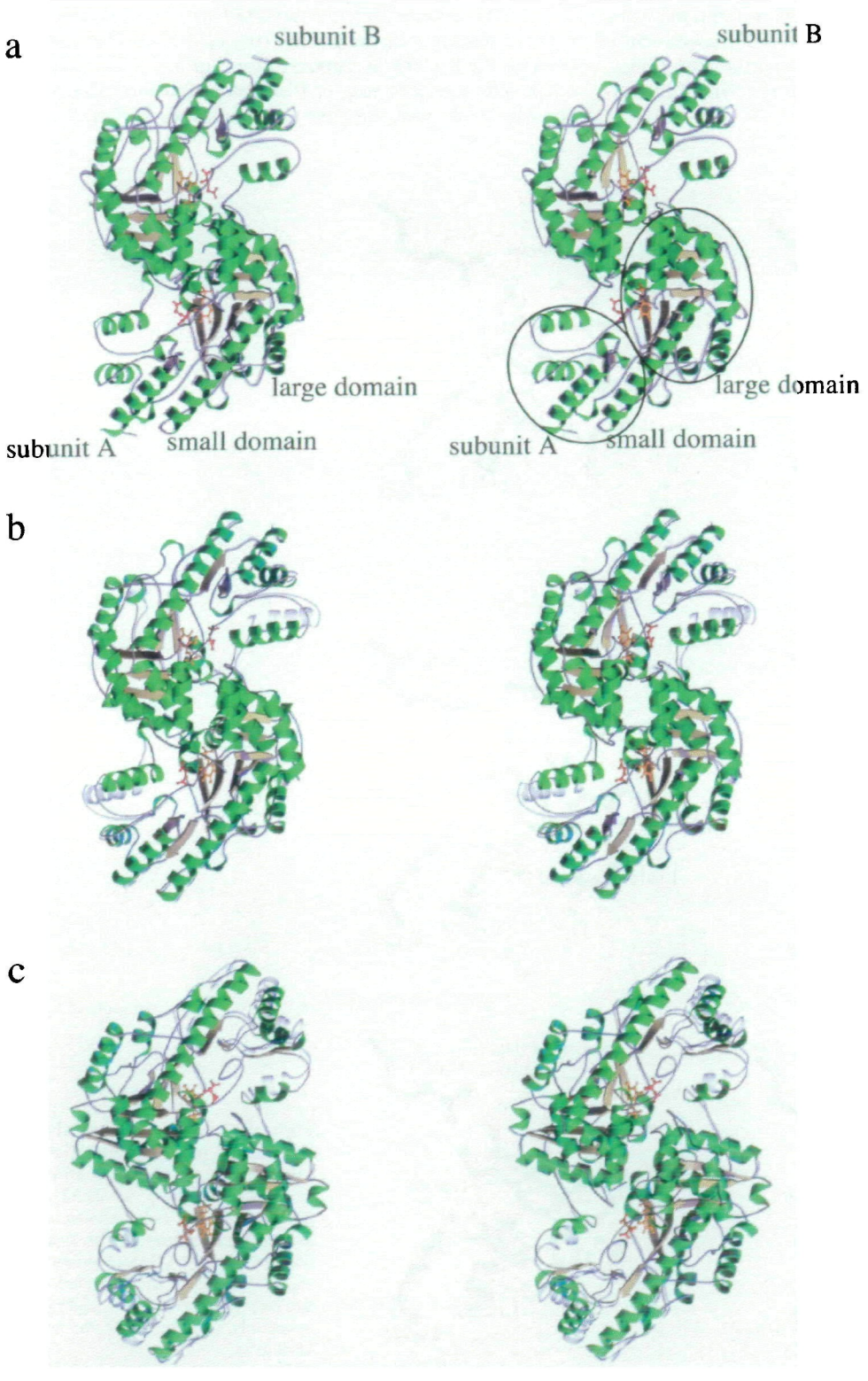

Fig. 1. **Stereo ribbon diagrams of the three aminotransferase molecules viewed down the 2-fold axis.** (a) PhAT (PDB code, 1GD9 and 1GDE). (b) TtAT (*14*; PDB code, 1BJW and 1BKG). (c) EcAT (*10*, *11*; PDB code, 1AMQ and 1AMR). The lower half of the molecule represents subunit A, and the upper half subunit B. The large and small domains of the lower subunit are circled. The labels are shown only in panel a. Each molecule in the liganded form is superimposed on the unliganded form by means of least-squares fitting of Cα atoms in the unchanged region (PhAT, 3rd–412th residues; TtAT, 31st–408th residues; EcAT, 49th–325th residues). The α-helices, β-sheets, PLPs, and substrate analogs in the liganded form are colored green, yellow, orange, and red, respectively. The unliganded form is colored gray.

shown in Fig. 1a. The new model of unliganded PhAT revealed that the region of Glu16–Ala25 formed an α-helix, whose conformation had not been identified previously. Secondary structure assignments with the program DSSP (*28*) also suggested that this region formed an α-helix.

X-Ray diffraction data for PhAT reconstituted with a glutamate analog, *N*-5′-phosphopyridoxyl-L-glutamate, were collected at 1.8 Å resolution. To compare the subunit structure of the glutamate form with that of the unliganded form of PhAT, the Cα atoms in the unliganded (colored gray) and complexed forms were superimposed (Fig. 1a). Very little change was observed between the two forms. The root-mean-square deviation between the whole atoms was 0.20 Å.

Active Site Structure of PhAT—The active site structure of PhAT reconstituted with the glutamate analog is shown in Fig. 2a. The N-terminal α-helix (Glu16–Ala25) moves close to the active site with a root-mean-square deviation of 0.36 Å, which is small compared with in the case of the α-helix comprising Lys13 to Val30 of TtAT (6.2 Å).

The α-carboxyl group of glutamate interacted with Arg386 (Fig. 2a) and Nδ2 of Asn194 (see PDB files; data not shown in Fig. 2a), as for the other α-aminotransferases. The distal carboxyl group interacted with N of Gly38 via a water molecule and the phenol ring of Tyr70*. The distance between Oε1 of the ω-carboxyl group and Cζ of Tyr70* was 3.5 Å. The pyridine ring of PLP rotated around the N1-C2 bond by 23.0°, and the phenyl ring of Phe140, which inter-

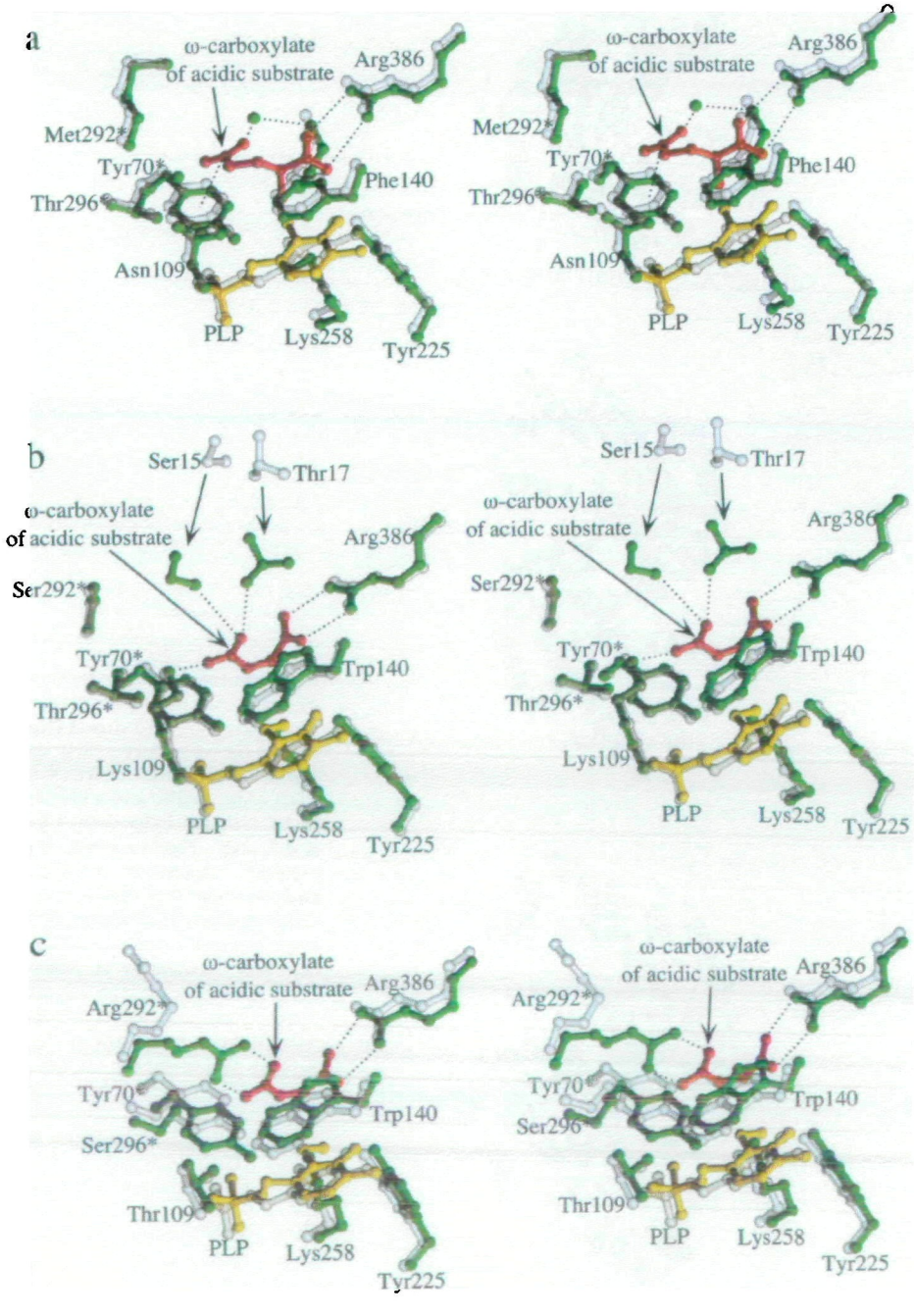

Fig. 2. **Stereodiagrams of the active sites of thermophilic and mesophilic aminotransferases.** (a) PhAT. (b) TtAT. (c) EcAT. Each panel shows an enlargement of the active-site structure in Fig. 1. Amino acid residues, PLP, and acidic substrate analogs in the liganded forms are colored green, yellow, and red, respectively. Unliganded forms are colored gray.

acts with PLP through ring-ring interaction, rotated in a similar way to in the case of PLP.

DISCUSSION

Differences in Recognition of an Acidic Substrate among PhAT, TtAT, and EcAT—Previously, we classified the pattern of recognition of carboxylate groups into four categories (*29*). In many cases (36%), positively charged Arg contributes to the recognition. Positively charged Lys (3%) and His (6%) are rare. The other residues, Asn, Gln, Trp, Ser, Thr, and Tyr, form hydrogen bonds (total 31%). The NH of the peptide backbone also participates in the recognition (22%). In the case of PhAT, the α-carboxylate group of the acidic amino acid substrate (glutamate) was recognized by Arg386, the recognition mechanism being identical to that in the case of TtAT or EcAT. The ω-carboxyl group was recognized by Tyr70* and a water molecule. The ω-carboxyl group might be protonated since the carboxyl group of model compounds is protonated in a hydrophobic environment with a dielectric constant lower than 20 (*30*, *31*). However, we can not rule out the possibility that the ω-carboxyl group of the glutamate moiety is forced to be in contact with the phenol group, because it is irreversibly bound with the coenzyme in the active site. This recognition mechanism of PhAT is quite different from that of TtAT and EcAT, where the positively charged Lys109 or Arg292*, respectively, recognizes the carboxylate group of the substrate.

Smaller Domain Movement with Increased Enzyme Thermophilicity—Upon binding of an acidic substrate to hyperthermophilic PhAT, little domain movement was observed (Figs. 1a and 2a). In the case of TtAT, only one helix, from Lys13 to Val30, showed significant movement to the bound substrate (Figs. 1b and 2b). A large conformational change occurred in EcAT (Fig. 1c and 2c). These differences among aminotransferases suggest that the more thermostable the enzyme is, the smaller its motion is. This may be a general rule for proteins as a whole, since the large fluctuation may cause enzymes to become unstable.

In order to verify this rule, we compared the movements of hyperthermophilic, extreme thermophilic, and mesophilic enzyme molecules upon binding to a substrate. The following two cases seem to fulfill the above criterion.

(A) The TATA-box-binding protein from hyperthermophilic *Pyrococcus woesei* does not change its conformation on binding to DNA (*32*; PDB code, 1D3U and 1PCZ), whereas a structural change was observed for mesophilic *Arabidopsis thaliana*, where one domain twists by 10° with respect to the other domain (*33*).

(B) The conformational change of aspartyl-tRNA synthetase from hyperthermophilic *Pyrococcus kodakaraesis* involves merely flipping out of the loop (residues 167–172), which changes the conformation from an open to a closed form to secure the aspartate residue in the active site (*34*; PDB code, 1B8A), whereas the anticodon binding domain (68–205) of mesophilic *Saccharomyces cerevisiae* undergoes a large rigid-body movement corresponding to a rotation of about 6° with respect to the catalytic module (*35*; PDB code, 1ASY and 1ASZ).

The results for these proteins support that thermophilic enzymes undergo small domain movements upon ligand binding, and that these small movements may be related to the stability of the proteins.

In conclusion, by comparing enzymes from a hyperthermophile, an extreme thermophile and a mesophile, we have found that they appear to obey a general rule: "the more thermophilic the enzyme is, the smaller the domain movement upon binding to a substrate is." It will be of considerable interest to determine whether this rule is applicable to the enzymes of psychrophiles.

We would like to thank Professor Emeritus N. Sakabe (National Laboratory for High Energy Physics), and Drs. N. Igarashi and M. Suzuki (High Energy Accelerator Research Organization) for their help in data collection through synchrotron radiation.

REFERENCES

1. Mehta, P.K., Hale, T.I., and Christen, P. (1989) Evolutionary relationships among aminotransferases. Tyrosine aminotransferase, histidinol-phosphate aminotranferase, and aspartate aminotransferase are homologous proteins. *Eur. J. Biochem.* **186**, 249–253
2. Davies, G.J., Gamblin, S.J., Littlechild, J.A., and Watson, H.C. (1993) The structure of a thermally stable 3-phosphoglycerate kinase and a comparison with its mesophilic equivalent. *Proteins* **15**, 283–289
3. Makhatadze, G.I. and Privalov, P.L. (1995) Energestics of protein structure. *Adv. Protein Chem.* **47**, 307–417
4. Vogt, G., Woell, S., and Argos, P. (1997) Protein thermal stability, hydrogen bonds, and ion pairs. *J. Mol. Biol.* **269**, 631–643
5. Kumar, S., Tsai, C.J., and Nussinov, R. (2000) Factors enhancing protein thermostability. *Protein Eng.* **13**, 179–191
6. Jaenicke, R. and Böhm, G. (1998) The stability of proteins in extreme environments. *Curr Opin. Struct. Biol.* **8**, 738–748
7. Hoseki, J., Yano, T., Koyama, Y., Kuramitsu, S., and Kagamiyama, H. (1999) Directed evolution of thermostable kanamycin-resistance gene: a convenient selection marker for *Thermus thermophilus*. *J. Biochem.* **126**, 951–956
8. Takano, K., Yamagata, Y., and Yutani, K. (1998) A general rule for the relationship between hydrophobic effect and conformational stability of a protein: stability and structure of a series of hydrophobic mutants of human lysozyme. *J. Mol. Biol.* **280**, 749–761
9. Takano, K., Yamagata, Y., Funahashi, J., Hioki, Y., Kuramitsu, S., and Yutani, K. (1999) Contribution of intra- and intermolecular hydrogen bonds to the conformational stability of human lysozyme. *Biochemistry* **38**, 12698–12708
10. Miyahara, I., Hirotsu, K., Hayashi, H., and Kagamiyama, H. (1994) X-ray crystallographic study of pyridoxamine 5′-phosphate-type aspartate aminotransferases from *Escherichia coli* in three forms. *J. Biochem.* **116**, 1001–1012
11. Okamoto, A., Higuchi, T., Hirotsu, K., Kuramitsu, S., and Kagamiyama, H. (1994) X-ray crystallographic study of pyridoxal 5′-phosphate-type aspartate aminotransferases from *Escherichia coli* in open and closed form. *J. Biochem.* **116**, 95–107
12. Ishijima, J., Nakai, T., Kawaguchi, S., Hirotsu, K., and Kuramitsu, S. (2000) Free energy requirement for domain movement of an enzyme. *J. Biol. Chem.* **275**, 18939–18945
13. Okamoto, A., Kato, R., Masui, R., Yamagishi, A., Oshima, T., and Kuramitsu, S. (1996) An aspartate aminotransferase from an extremely thermophilic bacterium, *Thermus thermophilus* HB8. *J. Biochem.* **119**, 135–144
14. Nakai, T., Okada, K., Akutsu, S., Miyahara, I., Kawaguchi, S., Kato, R., Kuramitsu, S., and Hirotsu, K. (1999) Structure of *Thermus thermophilus* HB8 aspartate aminotransfersase and its complex with maleate. *Biochemistry* **38**, 2413–2424
15. Matsui, I., Matsui, E., Sakai, Y., Kikuchi, H., Kawarabayasi, Y., Ura, H., Kawaguchi, S., Kuramitsu, S., and Harata, K. (2000) The molecular structure of hyperthermostable aromatic aminotransferase with novel substrate specificity from *Pyrococcus horikoshii*. *J. Biol. Chem.* **275**, 4871–4879

16. Severin, E.S., Gulyaev, N.N., Khurs, E.N., and Khomutov, R.M. (1969) The synthesis and properties of phosphopyridoxyl amino acids. *Biochem. Biophys. Res. Commun.* **35**, 318–323
17. Leslie, A.G.W. (1992) *Joint CCP4 and ESF-EACBM Newsletter on Protein Crystallography*, No. 26, Daresbury Laboratory, Warrington, UK
18. Collaborative Computational Project No.4 (1994) The CCP4 suite: programs from protein crystallography. *Acta Crystallogr.* **D50**, 760–763
19. Brünger, A.T. (1992) *X-PLOR (Version 3.1): A System for X-ray Crystallography and NMR*, Yale University Press Press, New Haven, CT
20. Navaza, J. (1994) AMoRe: An automated package for molecular replacement. *Acta Crystallogr.* **A50**, 157–163
21. Brünger, A.T., Kuriyan, J., and Karplus, M. (1987) Crystallographic R factor refinement by molecular dynamics. *Science* **235**, 458–460
22. Brünger, A.T. (1991) Simulated annealing in crystallography. *Annu. Rev. Phys. Chem.* **42**, 197–223
23. Engh, R.A. and Huber, R. (1991) Accurate bond and angle parameters for X-ray protein structure refinement. *Acta Crystallogr.* **A47**, 392–400
24. Jones, T.A., Zou, J.-Y., Cowan, S.W., and Kjeldgaard, M. (1991) Improved methods for building protein models in electron density maps and the location of errors in these models. *Acta Crystallogr.* **A47**, 110–119
25. Laskowski, R.A., McArthur, M.W., Moss, D.S., and Thornton, J.M. (1993) PROCHECK-A program to check the stereochemical quality of protein structures. *J. Appl. Crystallogr.* **26**, 283–291
26. Merritt, E.A. and Murphy, M.E.P. (1994) Raster 3D version 2.0. A program for photorealistic molecular graphics. *Acta Crystallogr.* **D50**, 869–873
27. Kraulis, P.J. (1991) MOLSCRIPT: a program to produce both detailed and schematic plots of protein structures. *J. Appl. Crystallogr.* **24**, 946–950
28. Kabsch, W. and Sander, C. (1983) Dictionary of protein secondary structure: pattern recognition of hydrogen-bonded and geometrical features. *Biopolymers* **22**, 2577–2637
29. Nobe, Y., Kawaguchi, S., Ura, H., Nakai, T., Hirotsu, K., Kato, R., and Kuramitsu, S. (1998) The novel substrate recognition mechanism utilized by aspartate aminotransferase of the extreme thermophile *Thermus thermophilus* HB8. *J. Biol. Chem.* **273**, 29554–29564
30. Aksnes, G. (1962) The electrostatic effects in the ionization of weak acids in water and water-dioxane mixtures. *Acta Chem. Scand.* **16**, 1967–1975
31. Hasted, J.B. (1973) in Water (Franks, F., ed.) Vol. 2, pp. 405–458, Plenum Press, New York–London
32. Kosa, P.F., Ghosh, G., DeDecker, B.S., and Sigler, P.B. (1997) The 2.1 Å crystal structure of an archaeal preinitiation complex: TATA-box-binding protein/transcription factor (II) B core/TATA-box. *Proc. Natl. Acad. Sci. USA* **94**, 6042–6047
33. Kim, J.L., Nikolov, D.B., and Burley, S.K. (1993) Co-crystal structure of TBP recognizing the minor groove of a TATA element. *Nature* **365**, 520–527
34. Schmitt, E., Moulinier, L., Fujiwara, S., Imanaka, T., Thierry, J.C., and Moras, D. (1998) Crystal structure of aspartyl-tRNA synthetase from *Pyrococcus kodakaraensis* KOD: archaeon specificity and catalytic mechanism of adenylate formation. *EMBO J.* **17**, 5227–5237
35. Sauter, C., Lorber, B., Cavarelli, J., Moras, D., and Giege, R. (2000) The free yeast aspartyl-tRNA synthetase differs from the tRNA (Asp)-complexed enzyme by structural changes in the catalytic site, hinge region, and anticodon-binding domain. *J. Mol. Biol.* **299**, 1313–1324